



Chloride migration and long-term natural carbonation on concretes with calcined clays: A study of calcined clays in Argentina

Gisela Cordoba^a, Ricarda Sposito^{b,*}, Mathias Köberl^b, Silvina Zito^a, Nancy Beuntner^b, Alejandra Tironi^a, Karl-Christian Thienel^b, Edgardo F. Irassar^a

^a Facultad de Ingeniería, CIFICEN (UNCPBA-CICPBA-CONICET), B7400JWI Olavarría, Argentina

^b Institut für Werkstoffe des Bauwesens, Universität der Bundeswehr München, 85577 Neubiberg, Germany

ARTICLE INFO

Keywords:

Calcined common brick clay
Calcined low-grade kaolinitic clay
Concrete
Chloride ingress
Carbonation

ABSTRACT

The use of calcined clays as supplementary cementitious materials is one of the strategies to reduce the CO₂ emissions from cement and concrete industry as they provide good mechanical and durable properties after proper calcination and grinding. In Argentina, calcined common brick clays have a significant relevance due to their proximity to the largest Portland cement plants. The aim of this study is to analyze the resistance to chloride ingress and natural carbonation up to 36 months of concretes using calcined common brick clay and calcined low-grade kaolinitic clay. The latter exhibits a much lower chloride migration coefficient than the Portland cement concrete from 28 days on, while the calcined common brick clay requires a 90 days curing to obtain lower chloride ingress. Although the blended concretes exhibit greater carbonation depths than the reference after 36 months, it is lower than the given threshold of 10 mm. Hence, durable concretes with calcined clay can be obtained if they are properly cured.

1. Introduction

Concrete structures are key to the built environment, being a fundamental part of housing, transport and energy generation infrastructure, and other essential structures for modern life [1]. Concrete widespread use is mainly due to its good mechanical performance, the facility to produce it with locally available materials, and its relatively low cost [1–3].

However, to meet the demands posed to curb climate change, it is necessary to reduce CO₂ emissions from the cement and concrete industry. Several actions are proposed in this regard, such as saving on clinker production (by means of the use of decarbonated raw materials, increasing thermal efficiency, etc.) or cement and binders (through Portland clinker cement substitution or alternatives to Portland clinker cement), increasing the efficiency in concrete production, design and construction (by optimizing mix and structural design, lifetime extension, etc.), decarbonization of electricity, re-carbonation, or carbon capture and utilization/storage [1–3].

According to the Global Cement and Concrete Association (GCCA), by optimizing the design of concrete structures, it is possible to reduce both costs and up to 22% of the CO₂ emissions of concrete, as it is possible to decrease the amount of materials used, to increase the application of reprocessed and recycled materials and to extend the lifetime, contributing to achieve the goal of net-zero concrete by 2050 [1].

* Corresponding author.

E-mail address: ricarda.sposito@unibw.de (R. Sposito).

<https://doi.org/10.1016/j.cscm.2022.e01190>

Received 21 February 2022; Received in revised form 28 April 2022; Accepted 20 May 2022

Available online 23 May 2022

2214-5095/© 2022 The Author(s). Published by Elsevier Ltd. This is an open access article under the CC BY license (<http://creativecommons.org/licenses/by/4.0/>).

Over the last decades, one of the most common durability problems in reinforced concrete structures has been related to reinforcement corrosion, which causes cracking, staining, and spalling of the concrete cover and leads to increased investment in maintenance and repair [4,5]. Changes in the pore solution, namely a reduction in pH value, are the driving forces when it comes to reinforcement depassivation and are mainly related to carbonation and chloride ingress [5,6]. Therefore, it is necessary to keep the porosity of the concrete as low as possible to reduce or slow the ingress of aggressive ions [2,5–7] and to increase the concrete cover to delay the ions from reaching the reinforcement [3].

The transport of chloride ions and CO₂ is closely related to the pore size, the connectivity of the pore structure, and its tortuosity [7, 8]. Therefore, transportation can be reduced or at least slowed down by refining the pore size in the cement matrix and disconnecting the porosity [2,7]. Furthermore, depending on the chemical composition of the cement, it is possible to reduce the ingress of chlorides by combination, either by Friedel's salt formation (chemical binding) or by adsorption into the hydrated phases of the cement (physical binding) [9–11]. Nevertheless, the carbonation depth depends not only on pore size and pore connectivity but also on the amount and type of carbonatable material and the changes in porosity due to the formation of carbonation products [8].

Different approaches are available to reduce the permeability of concrete, including low water-to-binder ratio (w/b), longer curing times, which increase the degree of cement hydration, or the use of pozzolanic supplementary cementitious materials (SCM), which can reduce pore size and disconnect the open porosity [2,3].

The use of SCM has been extensively adopted as it provides concretes with good mechanical and durable performance and reduces greenhouse gas (GHG) emissions from cement production [12,13]. Traditionally, granulated blast furnace slag, fly ash, and silica fume have been used as SCM. However, due to limited availability in some world regions, other materials have been studied as alternative SCM [14]. Calcined clays emerge as an attractive alternative due to their wide availability and pozzolanic activity when properly thermally activated [14–18]. Among the 2:1 clays, the illite/mica group is abundant in arid and high-latitude regions, being fairly abundant in both topsoil and subsoil in southern South America, central Europe, eastern North America, among other regions. While the kaolinite group is predominant in the humid tropics, being mostly abundant in northern South America, some regions of Africa and Asia [19].

In Argentina, Portland cement plants are geographically diversified, although about 50% of Portland clinker is produced in the district of Olavarría (Province of Buenos Aires). In this region, limestone is interbedded with layers of illitic clays, which the cement industry had not exploited until the last decade [20]. However, due to the abundance of illitic clays in quarries surrounding cement plants, the industry has given special emphasis to the production of these clays as SCM and a composite Portland cement (CEM V/A) with limestone filler and calcined illitic clay has been commercialized on the domestic market since 2018 [21]. There are also other types of clays available nearby cement plants, such as kaolin, smectite, montmorillonite, among others. However, due to their scarce availability or the importance of these clays in other domestic industries, they do not appear to constitute a suitable solution for the cement industry in Argentina.

The pozzolanic reaction of calcined clays reduces the availability of calcium hydroxide (CH) and increases the volume of hydrated phases (C-S-H, C-A-S-H, AFm) [17,22]. The partial replacement of Portland cement by calcined clays increases the total porosity of the cement paste, while their pozzolanic activity leads to a refinement of the pore size [16,23–26]. This increase in the volume of the hydrated phases and the pore size refinement can enhance the resistance to chloride ingress [11]. At the same time, the reduction of the available CH can ease the carbonation of the cement paste and lead to coarsening porosity due to carbonation shrinkage [8].

As the use of calcined clays as SCM may improve the concrete durability and extend the service life of reinforced concrete structures, it also enhances the concrete's environmental efficiency by reducing GHG emission, extending the time needed until the renovation of structures, and the subsequent reduction in the use of raw materials for their construction [2,5].

Within calcined clays, metakaolin and low-grade kaolinitic clays have been extensively studied [13,27,28], whereas 2:1 clays [16, 29] or intermixed clays are now studied in more detail [30,31]. However, most of the studies have been carried out on cement pastes and mortars, with an overview on concretes, especially using calcined kaolinitic clay. Due to the significance of calcined common brick clay and the existence of blended cements containing this type of clay commercialized in the Argentinian domestic market, further studies on the mechanical and durable performance of concretes containing such blended cements are needed.

This study analyzes the influence of porosity and water transport mechanisms on chloride ingress and natural carbonation of concretes using calcined common brick clay (containing illite as the principal mineral) and calcined low-grade kaolinitic clay, as processes that can induce corrosion of reinforcing bars. For that purpose, chloride migration of concretes cured 28 and 90 days and natural carbonation of concretes cured 7 and 28 days and exposed up to 36 months were studied.

2. Materials and testing procedure

2.1. Materials and mixtures

An ordinary Portland cement (OPC), type CEM I 42.5 N, complying with EN 197–1, and two calcined clays, namely a calcined common brick clay (BC) and a calcined low-grade kaolinitic clay (KC), were used. Clays were calcined in a laboratory muffle kiln. The calcination temperature was chosen depending on the main clay mineral to ensure correct dehydroxylation and formation of pozzolanic material: BC was calcined at 950 °C and KC, at 750 °C. BC was ground in a ball mill after calcination to obtain 90% of the particle size lower than 45 µm. Further information on the selection of calcination temperature and grinding of calcined clays was previously published by the authors [15,32].

Table 1 shows the chemical composition and physical characteristics of OPC, BC and KC, as well as the mineralogical composition of the raw and calcined clays. According to the data provided by the manufacturer, the mineralogical composition of the Portland

clinker is 63.6 % by mass (wt%) of C_3S , 15.1 wt% of C_2S , 2.8 wt% of C_3A , and 14.3 wt% of C_4AF . OPC further has 5 wt% gypsum and 3 wt% limestone as minor components. The raw common brick clay contains illite (47 wt%) as the main mineral, and the low-grade kaolinitic clay, kaolinite (46 wt%). Both clays contain quartz as the main impurity. After calcination, both calcined clays have a similar amorphous phase content (56/57 wt%). BC presents a high content of K_2O in its composition due to the presence of illite, while KC is rich in Al_2O_3 , which is characteristic of kaolinite.

The Blaine surface area of OPC is about half of that of BC and KC, with KC possessing the highest Blaine surface area. The BET-specific surface area was measured according to DIN ISO 9277. The BET-specific surface area, in contrast with the Blaine surface area, also considers the inner porosity of powder materials and is much higher for KC than for BC. The particle density of calcined clays is lower than that of the OPC. According to the particle-size distribution parameters, obtained by laser diffraction using a Malvern Mastersizer 2000, both calcined clays present a higher volume of small particles than the OPC.

The authors have proved the pozzolanicity of the calcined clays through the Frattini test in a previous paper [33]. In the present paper, the CH consumption by the calcined clays was measured in pastes with a 20 wt% replacement of OPC by BC and KC with $w/b = 0.50$ up to 90 days. The reference paste with OPC only is designated as P-OPC and the blended pastes as P-20BC and P-20KC, respectively. Thermogravimetric (TG) analyses were performed with Netzsch STA 449 F3 Jupiter with a heating rate of 2 K/min on samples stopped with acetone. The CH content (wt%) was calculated as the weight loss (WL_{CH}) between 400 and 550 °C according to Eq. (1), considering the molecular mass of CH ($m_{CH} = 74$ g/mol) and water ($m_w = 18$ g/mol) [34].

$$CH = WL_{CH} * \frac{74}{18} \quad (1)$$

Table 2 shows the CH content of the pastes. At 7 days, P-20BC and P-20KC contained 80% and 78% of the CH of P-OPC, respectively. The pozzolanic reaction of BC had not yet started since the lower CH content of P-20BC corresponds only to the dilution due to the replacement of OPC by the calcined clay. For P-20KC, an incipient pozzolanic reaction of KC was observed, as the reduction in CH content slightly exceeded the dilution of KC replacement.

At 28 days, the relative CH content in P-20BC and P-20KC corresponded to 76% and 70%, respectively. While the pozzolanic reaction of BC just had started, the one of KC had started within 7 days, which explains the higher CH consumption in P-20KC. At 90 days, the relative CH content in P-20BC and P-20KC corresponded to 68% and 57%, respectively. The CH content confirmed the pozzolanicity of BC and KC, with higher reactivity of KC, as the reaction starts earlier and consumes a higher proportion of CH.

Concretes were made with 25 wt% replacement of OPC by calcined clay and $w/b = 0.50$. The corresponding designations for the concretes were C-OPC, C-25BC and C-25KC. Natural silica sand from the Parana River (Argentina) was used as fine aggregate (fineness modulus = 2.35; density = 2.67 kg/dm³) and crushed granite from a quarry at Olavarría (Province of Buenos Aires, Argentina) as coarse aggregate (maximum nominal size of 16 mm; density of 2.70 kg/dm³; bulk density in a loose and compacted condition = 1430 and 1560 kg/m³, respectively). The content of silica sand was modified to offset the differences in density between the OPC and the calcined clays. Table 3 shows the concrete mix proportions. The granulometric curve of total aggregates met the AB16 curves stated in

Table 1
Chemical composition and physical properties of OPC and calcined clays.

Cement/Calcined clay	OPC	BC	KC
Chemical composition, wt%			
SiO ₂	20.6	66.3	71.7
Al ₂ O ₃	4.3	16.3	23.9
Fe ₂ O ₃	4.4	9.2	1.0
CaO	62.0	0.3	0.3
MgO	0.6	1.5	0.3
SO ₃	2.4	–	–
Na ₂ O	0.05	0.1	0.1
K ₂ O	1.2	5.6	0.7
LOI	1.7	0.6	0.5
Mineralogical composition of raw clays, wt%			
Kaolinite	–	–	46
Quartz	–	48	41
Illite	–	47	6
Hematite	–	5	–
Mineralogical composition of calcined clays, wt%			
Quartz	–	34	43
Illite	–	4	0
Hematite	–	6	0
Amorphous	–	56	57
Physical properties			
Specific surface area, m ² /kg	Blaine	622	708
	BET	–	18.1
Density, kg/dm ³	3.16	2.66	2.59
Particle size distribution parameters, μm	d ₁₀	3.30	2.23
	d ₅₀	20.51	10.66
	d ₉₀	54.36	60.48

Table 2
CH content of P-OPC, P-20BC, and P-20KC.

		P-OPC	P-20BC	P-20KC
CH content, wt%	7 days	16.6	13.4	12.9
	28 days	18.4	14.0	12.9
	90 days	21.8	14.8	12.5

DIN 1045–2 standard, with a fine aggregate/total aggregate ratio = 0.43.

A polycarboxylate-based superplasticizer (SP) (BASF, Trostberg, Germany) was used to guarantee the proper workability of the fresh concrete. The dosage was adjusted to obtain concretes within consistency S2 according to EN 206. The C-OPC superplasticizer dosage used was 0.24%, measured by weight of cementitious material. For C-25BC, it was almost not necessary to increase the dosage (0.25%). For C-25KC, the superplasticizer dosage (1.13%) was 370% higher than C-OPC, attributed to the higher particle fineness, BET and further physical characteristics of KC.

2.2. Testing procedure

Concrete characterization was carried out through compressive strength (EN 12390–3:2020) at 7, 28, and 90 days. The pore size distribution on comparable pastes (P-OPC, P-25BC, and P-25KC) was determined by using a mercury intrusion porosimeter (Thermo Scientific Pascal 140 and 440, Waltham, Massachusetts) complying with DIN 66133, at 28 and 90 days. From the pore size distribution curve, the cumulative pore volume and the pore size threshold were determined. According to the pore diameter, porosity can be classified as capillary pores and gel pores. From the capillary porosity, it is possible to distinguish between large capillaries (10–0.05 μm) and medium capillaries (50–20 nm). Gel pores can be classified as small capillaries (10–2.5 nm), micropores (2.5–0.5 nm) and micropores “interlayer” (<~0.5 nm) [35].

Water transport properties of concretes were studied through water absorption and permeable voids volume (ASTM C 642). The rate of water capillary absorption (sorptivity) (ASTM C 1585) was determined using cylinders (100 mm diameter and 50 mm height) cured 7, 28, and 90 days. According to ASTM C 1585, it is possible to determine two capillary absorption rates: an initial one, between 0 and 6 h, and a secondary one, after 6 h. Under this standard, the correlation value of the trend line must be $R^2 \geq 0.98$ for the capillary absorption rate to be valid. The water penetration under pressure was measured using 150 mm cubes cured 28 and 90 days.

Chloride migration (NT Build 492) in cylinders (100 mm diameter and 50 mm height) cured for 28 and 90 days. For the chloride migration test, the average of two specimens was calculated. The cylinders were cut from the half-height of the 200 mm height specimens, exposing that face to the chloride solution. Once the test time was completed, the specimens were split, sprayed with silver nitrate indicator solution, and the depth of chloride ingress was measured. Then, the chloride migration coefficient (D_{nssm}) was determined according to Eq. (2), where T is the average value of the initial and final temperatures in the anolyte solution ($^{\circ}\text{C}$), L is the thickness of the specimen (mm), U is the applied voltage (V), t is the test duration (hour), and x_d is the average value of the penetration depths (mm):

$$D_{nssm} = \frac{0.0239}{(U-2)} \frac{(273+T)}{t} L \left(x_d - 0.0238 \sqrt{\frac{(273+T)}{U-2}} \frac{L}{U-2} x_d \right) \quad (2)$$

Natural carbonation was measured after 3, 6, 12, 24, and 36 months of exposition in concrete specimens cured for 7 and 28 days in a rural area (CO_2 concentration of 350–400 ppm) on prismatic specimens with 100 mm height and 70 mm side length. Prisms were placed with the molding and lateral faces exposed to air and rain. The carbonation depth was determined on a sawn section of the concrete prisms, using a phenolphthalein solution as a pH indicator. This paper reports the average carbonation depth on the molding face since it is the face in practice exposed to carbonation where the highest depth is measured in all concretes. For the average calculation, the carbonation depth was measured between 10 and 60 mm of the molding face to avoid maximum values affected by the wick effect of the edge of the specimen and measured every 5 mm (taking into account 11 values for each specimen).

The carbonation coefficient (k) at the molding face was calculated based on Fick’s first law, from which Eq. (3) is derived [36]. Here, X_c is the carbonation depth (mm) at a given time, and t is the given time (years).

$$k = \frac{X_c}{\sqrt{t}} \quad (3)$$

Table 3
Concrete mix proportion.

	C-OPC	C-25BC	C-25KC
Concrete mixture proportion, kg/m^3			
Cementitious material	350	350	350
Water	175	175	175
Coarse Aggregate	1050	1050	1050
Natural silica sand	807	805	788
SP (% by mass of cement)	0.24	1.13	0.25

3. Results and discussion

3.1. Compressive strength

Table 3 shows the compressive strength of concretes at 7, 28, and 90 days. At 7 days, the compressive strength of the concretes made with blended cement was lower than the reference concrete. The compressive strength of C-25BC was 87% and 94% compared to that of C-OPC at 28 and 90 days, respectively. For C-25KC, the compressive strength surpassed the corresponding C-OPC at 28 days already, being 115% and 114% at 90 days, respectively. Nonetheless, it was for both higher than 75% of the C-OPC strength, which indicated already a contribution of BC and KC. The different behavior of the concretes with calcined clays was attributed to the higher reactivity of KC compared to BC.

3.2. Porosity

Fig. 1 shows the pore size distribution for P-OPC, P-25BC, and P-25KC cured 28 and 90 days. Total porosity and pore size threshold are presented in Table 3. Blended cement pastes exhibited a higher total porosity than the Portland cement paste at both measured ages. This mainly related to the higher volume of medium capillary pores in pastes made with blended cement. P-25BC showed a significantly higher pore size threshold than P-OPC and P-25KC at 28 days (55% and 100% higher, respectively), reaching at 90 days a pore size distribution similar to that of P-OPC at 28 days. P-25KC, despite having a higher total porosity than P-OPC, exhibited a lower pore size threshold at both 28 and 90 days (33% and 50% lower, respectively).

The increase in total porosity of pastes with blended cement is attributed to the dilution effect caused by the replacement of OPC for calcined clays [37]. However, the pozzolanic reaction of BC and KC led to pore size refinement, which confirmed earlier finding, e.g., in [22,24,38]. Moreover, the pore size refinement reduced the pore size threshold due to a decrease in large capillary pores and an increase in small capillary pores. Likewise, the age at which the reduction of the pore size threshold occurred depended on the reactivity of the calcined clay. For P-25KC, it occurred within the 28 days, while for P-25BC, it occurred later, between 28 and 90 days.

3.3. Water transport properties

Table 4 provides the water absorption, the permeable voids volume, and the initial absorption rate of concretes cured for 7, 28, and 90 days and the water penetration of concretes cured for 28 and 90 days.

At 7 days, the water absorption of concretes with blended cement was higher than for the C-OPC. At 28 and 90 days, the water absorption was equivalent among the concretes, with slightly higher values in the blended cement concretes.

The permeable voids volume represents the open porosity and depends mainly on the pore size of the cement matrix and partly on the porosity of the interfacial transition zone (ITZ) [35,39]. It did not change significantly between 7 and 90 days neither, neither for C-OPC nor for C-25KC. For C-25BC, the permeable voids volume was higher than C-OPC and C-25KC at 7 days (14%), whereas it reached equivalent values at 90 days.

Fig. 2 shows the sorptivity curve of concretes cured for 7, 28, and 90 days. It depends on the open porosity of concrete and the pore size distribution of the cement matrix [2]. The initial absorption rate (SI) decreased between 7 and 28 days for all concretes. C-25KC (Fig. 2c) presented the lowest SI at 7 and 28 days, 52% and 56% lower than C-OPC (Fig. 2a), respectively. The most significant reduction between 7 and 28 days was observed for C-25BC (35%, Fig. 2b), followed by C-OPC (20%). At 90 days, the SI was similar for all concretes (Table 4). The secondary absorption rate could not be determined since $R^2 < 0.98$ in most cases, making the values obtained not valid according to ASTM C 1585.

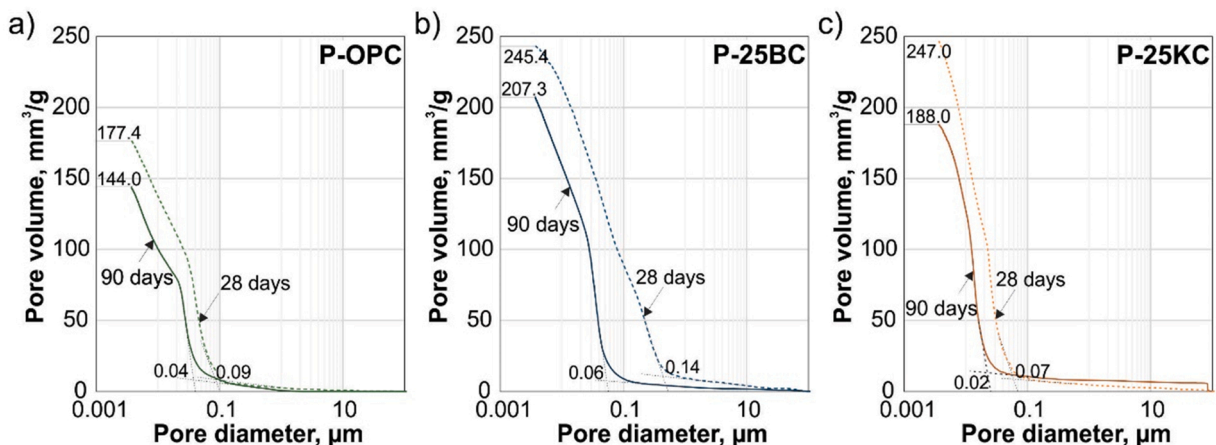


Fig. 1. Pore size distribution of a) P-OPC, b) P-25BC, and c) P-25KC at 28 and 90 days (dashed- and full-line, respectively).

Table 4
Hardened concrete properties for C-OPC, C-25BC, and C-25KC.

Property	Age, days	C-OPC	C-25BC	C-25KC	
Compressive strength, MPa	7	28.2	25.0	25.5	
	28	32.4	28.3	37.4	
	90	41.0	38.4	46.6	
Total porosity in paste, mm ³ /g	28	177.4	245.4	247.0	
	90	144.0	207.3	188.0	
Pore size threshold, μm	28	0.09	0.14	0.07	
	90	0.04	0.06	0.02	
Water absorption, %	7	4.8	5.5	5.4	
	28	4.6	4.9	4.9	
	90	4.5	4.7	4.7	
Permeable voids volume, %	7	11.9	13.6	12.0	
	28	10.9	11.7	11.1	
	90	10.5	11.0	11.0	
Initial absorption rate, mm/s ^{1/2}	7	13.1	18.6	6.3	
	28	10.5	12.0	4.6	
	90	4.6	4.2	4.7	
Water penetration, mm	28	Average	19.5	39.4	11.1
		Minimum	26.0	52.6	15.8
		Maximum	12.0	26.5	6.0
	90	Average	13.8	20.4	12.9
		Minimum	17.0	30.7	14.8
		Maximum	10.9	11.9	10.1

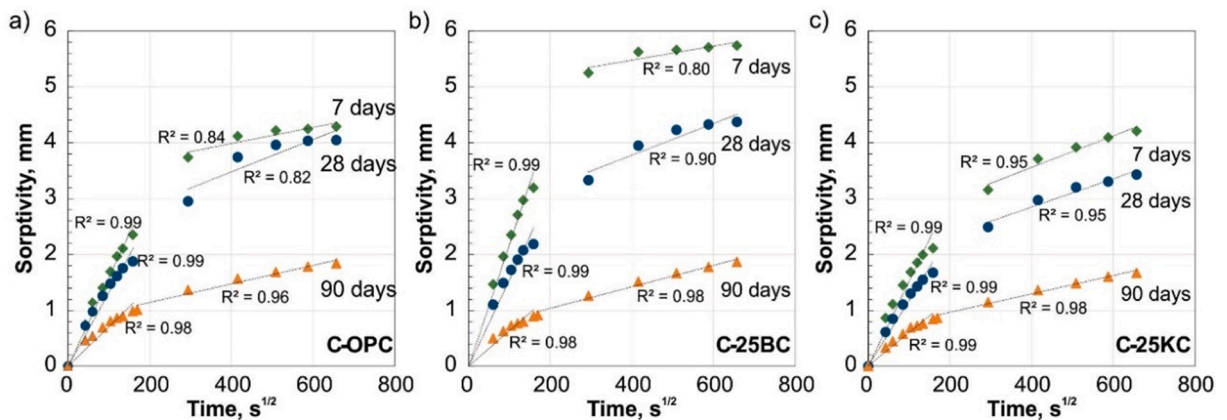


Fig. 2. Sorptivity of a) C-OPC, b) C-25BC, and c) C-25KC at 7, 28, and 90 days.

The average *water penetration* of C-25BC was the highest at both 28 and 90 days, being 100% and 48% higher than C-OPC at the respective ages. For C-25KC, the average water penetration was the lowest at 28 and 90 days, 43% and 6% of C-OPC values, respectively. The reduction in water penetration of C-OPC was about 30% between 28 and 90 days, about 50% for C-25BC, the reduction was about 50% and negligible for C-25KC due to the low water penetration already at 28 days.

Based on the present results, the effect at the different test ages of calcined brick clays and calcined kaolinic clays on the water transport properties of concretes can be summarized as follows:

- At 7 days, the dilution effect prevailed due to the partial replacement of OPC by BC and KC, which increased the water absorption of blended cement concretes. Dilution occurs due to the increase in the effective w/b ratio [37] and can be compensated by the increase in early hydration of the OPC due to the presence of fine particles [40] or the pozzolanic action of calcined clays. At this age, dilution was not compensated, leading to an increased total volume of capillary pores. On the other hand, the capillary absorption rate is related to the pore size and the interconnectivity of the pore network. The presence of fine particles may act as inert filler, blocking the pore network and decreasing the amount of interconnected pores [41]. The initial absorption rate of C-25KC was significantly lower than that of C-OPC, which was attributed to the disruption of the pore network by the presence of KC particles and to the incipient pozzolanic activity of this clay, which leads to the beginning of pore size refinement. BC did not act as an inert filler and neither showed pozzolanic activity at 7 days (Table 2), thus in C-25BC the dilution effect predominated and the capillary absorption rate was higher than in C-OPC.
- At 28 days, C-25BC had a slightly higher permeable pore volume than C-OPC, a 14% higher initial absorption rate, and twice the water penetration compared to C-OPC. In contrast, C-25KC had a pore volume equivalent to that of the C-OPC and its initial

absorption rate and water penetration were significantly lower than those of C-OPC. As shown in Table 4, the pozzolanic reaction of KC had already been ongoing at 7 days, while the pozzolanic reaction of BC started between 28 and 90 days. Consequently, the dilution effect dominated the water transport of C-25BC, which presented a more open pore structure and larger capillary pore size (Fig. 1). At this age, however, the pozzolanic reaction of KC produced a refinement and disconnection of the pore network that reduced the water transport in the concrete.

- At 90 days, the water absorption, permeable void volume, and initial absorption rate of blended cement concretes were all equivalent to C-OPC. However, P-25BC presented a pore size threshold in the cement matrix and water penetration similar to P-OPC at 28 days. P-25KC had a higher total pore volume in the cement matrix than P-OPC, despite a lower pore size threshold and significantly lower water penetration of C-25KC than of C-OPC. The remarkable reduction of water transport in C-25BC between 28 and 90 days was attributed to the development of the pozzolanic reaction driving to the refinement of the pore structure and the reduction of the capillary pore size. For C-25KC, the water transport properties did not vary significantly between 28 and 90 days. This was attributed to the early start of the pozzolanic reaction of KC, which, although its progress continued towards 90 days, disconnected the open porosity earlier.

Therefore, the progress of cement hydration and the pozzolanic reaction in blended cement both cause a denser microstructure due to physicochemical effects. In the first place, the replacement of cement by calcined clay interrupts the capillary pores (physical effect) [41]. In the second place, the pozzolanic reaction and the formation of secondary hydration products (AFm and C-S-H phases) refine the pore size and decreases the pore size threshold [25,30,42] as well as densifies the ITZ [39,43]. These benefits are obtained at different ages, depending on the reactivity of the calcined clay, and modify the water transport properties of the concretes.

3.4. Durability-related parameters that can induce corrosion of reinforcement bars

3.4.1. Chloride ingress

Fig. 3 shows the D_{nssm} of concretes cured for 28 and 90 days. At 28 days, C-25BC exhibited the highest coefficient ($21.1 \times 10^{-12} \text{ m}^2/\text{s}$), about 68% higher than C-OPC ($12.7 \times 10^{-12} \text{ m}^2/\text{s}$). In contrast, C-25KC yielded the lowest coefficient ($1.6 \times 10^{-12} \text{ m}^2/\text{s}$), which indicated a reduction by 88% compared to C-OPC.

At 90 days, the D_{nssm} of C-25BC was 75% lower than it was at 28 days ($5.2 \times 10^{-12} \text{ m}^2/\text{s}$) and lower than C-OPC ($8.5 \times 10^{-12} \text{ m}^2/\text{s}$). Meanwhile, the already significantly lower D_{nssm} of C-25KC hardly decreased between 28 and 90 days ($1.5 \times 10^{-12} \text{ m}^2/\text{s}$).

The resistance to chloride ingress is usually related to the pore size and the connectivity of the concrete porosity [11,44–46]. However, a good correlation between chloride ingress and pore size/pore connectivity was observed when comparing the same cement type. For different types of cement, the correlation levels drop, suggesting that the resistance of concrete to chloride ingress is not only dependent on porosity [47]. The ability of the hydrated phases of the cement to bind chlorides, either by physical binding (adsorption in the AFm phases or C-S-H) or by chemical binding through Friedel's salt formation may also increase the resistance to chloride ingress of concrete [9,44,48,49]. In this kind of short, non-steady-state chloride migration test, a reduced chloride combination condition is present [50]. Hence, the chemical combination of chlorides is considered practically negligible and it is assumed that chloride binding will be mainly by adsorption on the hydrated phases.

C-25KC had an excellent resistance towards chloride ingress from 28 days on. C-25BC instead only performed well if cured for an extended period. Both calcined clays possessed a similar amorphous phase content (Table 1), which was available to react with the CH during the pozzolanic reaction. However, KC had a higher aluminum content available in the amorphous phase than BC, favoring a higher formation of AFm phases in C-25KC than in C-25BC. The formation of C-S-H and AFm phases during the pozzolanic reaction drives to the space filling and to a greater pore size refinement. Then, in C-25KC there was a combination of a reduction in pore size (Fig. 1c) and a higher amount of hydration products formed by the pozzolanic reaction (Table 2). For C-25BC, the dilution effect remained noticeable at 28 days, as the cement paste had a larger pore size than the OPC paste (Fig. 1a and b) and the pozzolanic reaction was incipient (Table 2). However, after 90 days of hydration, the pozzolanic reaction was evident in BC (Table 2). It increased

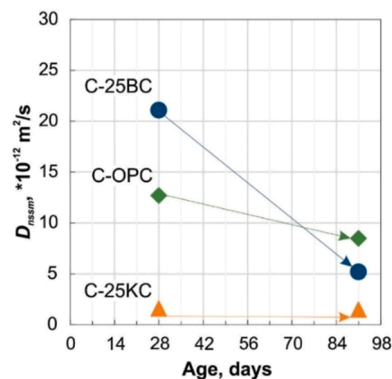


Fig. 3. Chloride migration coefficient (D_{nssm}) of concretes, at 28 and 90 days.

the hydrated phases content, leading to the pore size refinement and favoring to the physical binding of chlorides. For C-25BC cured for 90 days, the role of higher hydrated phase formation in the physical binding of chlorides was evident: in spite of the water penetration of C-25BC was higher than that of C-OPC and the cement paste with BC had a higher pore size distribution than the OPC paste, the D_{nssm} of C-25BC was in total lower than that of C-OPC.

The relationship of transport properties and D_{nssm} confirmed the correlation between relevant pore size, open porosity and chloride ingress resistance of concretes. Fig. 4a shows the correlation between pore-size threshold and D_{nssm} . A fairly good correlation is observed ($R^2 \sim 0.73$) for all concretes and curing regimes. However, C-25KC cured for 28 days slightly diverged from the tendency, as it exhibited a very low D_{nssm} already at 28 days. If C-25KC cured for 28 days is excluded from the calculation, a very good correlation ($R^2 \sim 0.91$) between pore-size threshold and D_{nssm} is obtained (Fig. 4b). This was attributed to the more pronounced formation of hydrated phases in C-25KC due to the early pozzolanic activity of KC, which contributed more to lowering D_{nssm} than to reducing the pore-size threshold.

On the other hand, water penetration is controlled by pore size and open porosity [51] and a good correlation is observed between that parameter and the D_{nssm} ($R^2 \sim 0.80$), respectively (Fig. 4b). Nevertheless, the ability of the concretes to adsorb chlorides influenced the correlation between the transport properties and the D_{nssm} . Fig. 4b shows that the points above the tendency line corresponded to the C-OPC, while the concretes with blended cement were below it. This indicated that, although the concretes with calcined clays showed higher water penetration rates (related to the pore size and open porosity) than the C-OPC, their D_{nssm} was lower. It was explained by the larger proportion of AFm phases formed due to the higher alumina content in blended cements with calcined clays, and the pozzolanic reaction that led to a higher C-S-H formation in such cement. Consequently, chloride adsorption in the hydrated phases increased and D_{nssm} decreased.

Hence, the lower performance of C-25BC at 28 days was attributed to the large pore size. At 90 days, the combined effect of lower porosity and physical chloride binding in the concrete mass contributed to the enhanced resistance to chloride ingress of C-25BC. For C-25KC, its excellent performance was attributed to the low porosity from 28 days (Fig. 1) and the physical chloride binding in the concrete mass.

3.4.2. Carbonation

Fig. 5 shows the average carbonation depth of concretes cured for 7 days (full line) and 28 days (dashed lines) from 3 to 36 months of exposure. The carbonation depth increased with time, regardless of the type of concrete and curing time. Nevertheless, it increased more in concretes with calcined clays than in C-OPC. On the other hand, the increase in curing time reduced the carbonation depth for all concretes.

C-OPC exhibited the lowest carbonation depth. For C-OPC cured for 7 days, the carbonation front hardly increased between 12 and 36 months and for C-OPC cured for 28 days, the carbonation depth barely changed between 24 and 36 months. C-25BC exhibited the highest carbonation depth at all ages for 7 and 28 days of curing. For C-25BC and C-25KC cured for 7 days, the carbonation depth was 175% and 153% higher than the one for C-OPC, respectively. For C-25BC and C-25KC cured for 28 days, the carbonation depth was 180% and 144% higher than the corresponding C-OPC, respectively.

Therefore, the presence of calcined clays impaired the carbonation resistance for both good (7 days) and very good potential curing (28 days). The lower CH content of concretes with calcined clays, due to the pozzolanic reaction, reduced the buffering capacity of this hydrated phase [8,52–54]. As a result, instead of carbonating CH in the first place, other hydrated phases (C-S-H, C-A-S-H, the AFm) were destabilized, leading to coarser porosity and increasing the diffusivity of CO_2 within the concrete mass [8,55,56]. While in Portland cement concretes, CH acted as buffer material and the calcite formation led to pore blocking and densification of the microstructure [8,52,54,57].

Fig. 6 shows the carbonation coefficient (k) of concretes at 3, 6, 12, 24, and 36 months of exposure, as calculated according to Eq. (3). It was higher in concretes with shorter curing, regardless of the concrete type and exposure time. Longer curing time led to the

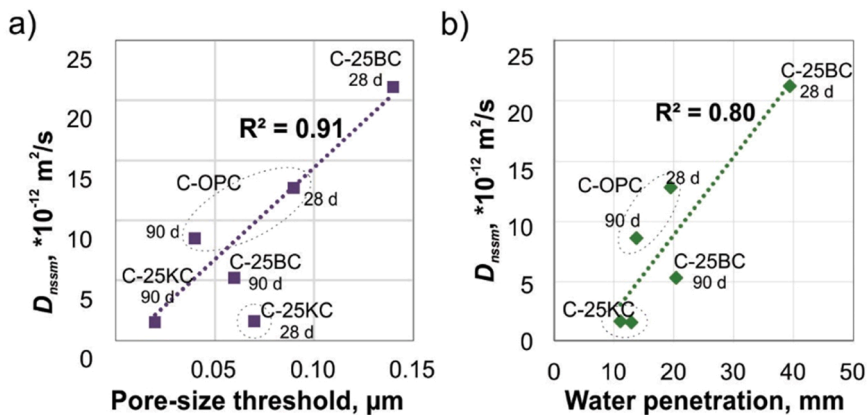


Fig. 4. Correlation between water transport properties and chloride migration coefficient (D_{nssm}). a) Pore-size threshold vs. D_{nssm} , b) Water penetration vs. D_{nssm} .

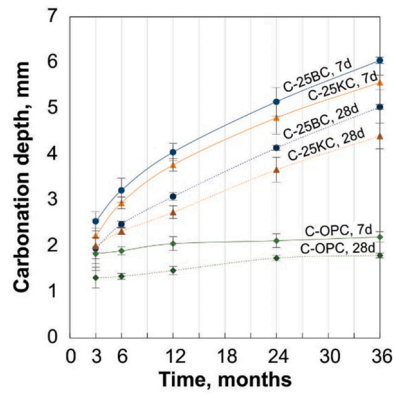


Fig. 5. Carbonation depth at the molding face of concretes cured 7 days (full line) and 28 days (dashed line) from 3 to 36 months of exposure in a rural area.

refinement of the cement paste porosity due to the progress of hydration, reducing k value [8]. Furthermore, within the concretes with calcined clays, C-25KC presented a lower k value than C-25BC, which was attributed to the reduction of the open porosity due to the earlier pozzolanic reaction of KC.

With progress in time, the k value decreased and the curves gradually became horizontal at around 24–36 months. The reduction of the k value over time was attributed to changes in porosity due to the precipitation of carbonation products by the reaction of CO_2 with the hydrated products [8,58]. At the same time, a significant reduction of the k value was observed in C-OPC, both cured for 7 and 28 days. This was mainly attributed to the large formation of calcite [8].

Moreover, the k value decreased more significantly in concretes cured for 7 days than in those cured for 28 days, regardless of the type of concrete. This was attributed to the higher maturation of the cement paste in the 28 days' cured concretes, which led to a pore size refinement and decreased the alteration of the porosity as a consequence of carbonation shrinkage.

The carbonation process is related to the water transport mechanisms of concrete, in particular to the open porosity. However, the chemical composition of the cement significantly affects the carbonation products formed and, consequently, the evolution of porosity over time [8]. For this reason, there was no good correlation between the different water transport parameters and the k value since the pozzolanic reaction of calcined clays affected the carbonation process. However, if C-OPC is excluded from this analysis and only concretes with calcined clays are considered, a fairly good correlation between permeable voids volume and the initial absorption rate with k value is obtained ($R^2 = 0.73$ and 0.64 , respectively), as shown in Fig. 7a and b. Therefore, the increased formation of C-S-H/C-A-S-H and AFm phases, simultaneously with the reduction of CH due to the pozzolanic activity, in blended cements had a similar effect on the carbonation resistance of C-25BC and C-25KC.

Despite the higher carbonation coefficient of concretes with calcined clays, the carbonation depth was less than 10 mm at 36 months in all concretes. According to EN 1992-1-1:2004, a concrete cover of 25 mm is required for structures under corrosion induced by carbonation, considering concrete surfaces subject to water contact and a structural class of S4. Thus, in combination with a k value of 1.27, 3.49, and 3.22 $\text{mm}/\text{year}^{1/2}$ for C-OPC, C-25BC, and C-25KC even cured for 7 days, respectively, the carbonation front would reach the reinforcing bars at 50 years or more, which indicates a good performance for all concretes.

The effect of using calcined brick clay and calcined kaolinitic clay to chloride ingress and carbonation resistance of concretes can be summarized as follows:

- Resistance to chloride ingress is closely related to porosity, both pore size and open porosity. However, the ability of the cement matrix to bind chlorides also affects it. C-25BC exhibited a higher chloride migration coefficient than C-OPC at 28 days, mainly due to the higher pore size threshold and open porosity. However, a drastic reduction was observed at later ages (90 days), attributable to the reduction in porosity and the increased formation of hydration products formed by the evolution of hydration and pozzolanic activity, which occurred between 28 and 90 days. For C-25KC, a very low chloride migration coefficient was observed from 28 days on due to its low pore-size threshold and the large volume of hydration products formed by the pozzolanic reaction between 7 and 28 days. However, despite increasing resistance to chloride ingress, CH consumption in C-25BC and C-25KC could have a detrimental effect on corrosion by chlorides, as it provides a buffering capacity to the concretes. On the one hand, CH maintains the high pH of the pore solution, and on the other hand, it inhibits local acidification and consequently pitting corrosion [54,59]. Therefore, the resistance to corrosion by chloride ingress in concretes with calcined clays depended on the curing, the composition of the mix and the moisture conditions of the particular application [54].
- Carbonation depends on the open porosity of concrete, the CH content of the cement matrix and the changes in porosity caused by the reaction of CO_2 with the hydration products. Hence, if carbonation products block the porosity of the concrete, carbonation will decrease as the exposure time increases. On the contrary, if carbonation-related shrinkage occurs, the pore size increases, the CO_2 can ingress more easily, and the carbonation continues into the concrete mass. The use of calcined clays increased the carbonation of concretes since the pozzolanic reaction reduced the CH content [52,57] and the carbonation products did not entirely block the

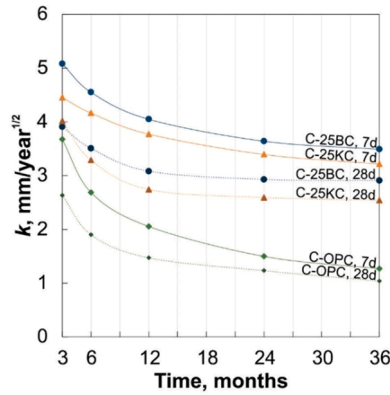


Fig. 6. Carbonation coefficient (k) of concretes cured for 7 days (full line) and 28 days (dashed line) from 3 to 36 months of exposure.

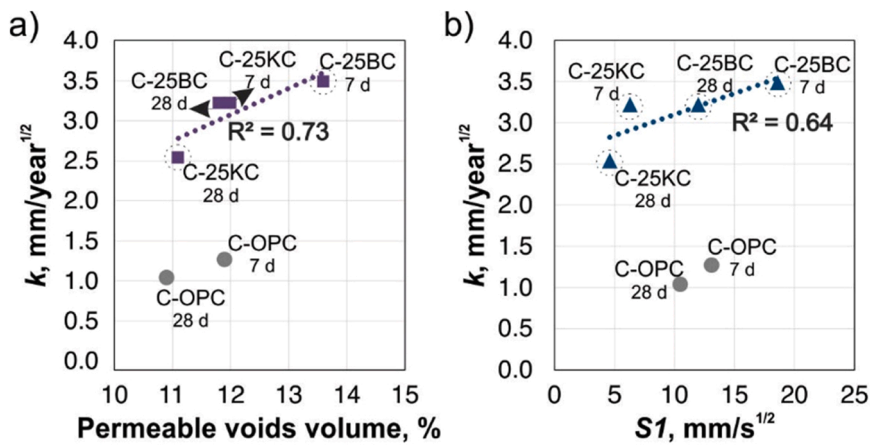


Fig. 7. Correlation between water transport properties and carbonation coefficient (k). a) Volume of permeable voids vs. k value, b) Initial absorption rate ($S1$) vs. k value.

pore structure as it was the case in C-OPC, which allowed higher CO₂ ingress [8,45,58]. However, the concretes exhibited carbonation depths < 10 mm up to 36 months, indicating an excellent performance of all of them.

4. Conclusions

This study compared the behavior of calcined clay blended concretes regarding to two durability parameters: chloride migration test and long-term natural carbonation. For the first time, a calcined common brick clay (BC), with illite as main mineral, was compared with a well-investigated, calcined low-grade kaolinitic clay (KC). BC has a significant industrial importance in Argentina, since it is extensively available in the area of the biggest cement plants. The different mineralogical composition of calcined clays impacts significantly their effect on water transport mechanism and durability parameters of concretes.

The total porosity, measured by MIP, was higher in pastes with calcined clays than in the reference paste. However, pore size refinement took place at an age of 28 days for P-25KC and was significantly observed towards 90 days of curing for P-25BC. As consequence, water absorption and permeable voids volume were both higher in concretes with calcined clays, where water absorption was not influenced by the type of calcined clay and the permeable voids volume was higher for C-25BC. Overall, the water transportation properties and the resistance to chloride ingress were both intimately related to the open porosity and were affected by the pozzolanic reaction of the calcined clays. In C-25BC, the reduction in water transport was observed after 28 days, and in C-25KC, it was observed from earlier ages. C-25KC exhibited a much lower chloride migration coefficient than C-OPC from 28 days on, whereas for C-25BC, the chloride migration coefficient was higher than C-OPC at 28 days and decreased notably towards 90 days, being eventually lower than the corresponding one of C-OPC.

The concretes with calcined clays exhibited after 36 months of natural carbonation greater carbonation depths than the C-OPC, due to the higher total porosity, the lower CH content and modifications in hydration products. On the other hand, extended curing times could reduce the carbonation depth. Especially concrete with calcined brick clay requires prolonged curing to attain similar or superior durability-related parameters compared to Portland cement concrete due to the later age, at which the pozzolanic reaction occurs.

Even though the concretes with calcined clays showed a lower performance than the Portland cement concrete, all the concretes investigated exhibited an excellent performance against carbonation. The estimated time to reach the reinforcing bars was at least 50 years.

Further research is needed on the use of ternary blended cements containing calcined common brick clay and limestone filler (LC3), to determine the effect of the combination of these SCMs on mechanical and durable properties of concretes. Additionally, sustainability of LC3 concretes should be analyzed in regions with a limited supply of traditional SCMs, such as Argentina.

Declaration of Competing Interest

The authors declare that they have no known competing financial interests or personal relationships that could have appeared to influence the work reported in this paper.

Acknowledgements

This research has been made possible with the CONICET (Argentina) - BAYLAT (Germany) cooperation initiative and the scholarship and support program for foreign students and doctoral candidates (STIBET), funded by the German Academic Exchange Service (DAAD) and the Universität der Bundeswehr München, awarded to Gisela Cordoba for a 3.5-month stay at the Universität der Bundeswehr München after 'Institut für Werkstoffe des Bauwesens. The Argentine researchers acknowledge the support received by the CICPBA and CONICET (PIO-004) and the Universidad Nacional del Centro de la Provincia de Buenos Aires (Project E02/122). They are also grateful to Loma Negra CIASA and Piedra Grande SA for the materials supplied. We acknowledge financial support by Universität der Bundeswehr München.

References

- [1] Global Cement and Concrete Association, Roadmap for Net Zero Concrete, 2021. (<https://gccassociation.org/concretefuture/wp-content/uploads/2021/10/GCCA-Concrete-Future-Roadmap.pdf>).
- [2] M.G. Alexander, A. Bentur, S. Mindess. *Durability of concrete*, first ed., Taylor & Francis, Boca Raton, USA, 2018.
- [3] P.-C. Aïtcin. *Binders for durable and sustainable concrete*, first ed., Taylor & Francis, Abingdon, UK, 2007.
- [4] A. Bentur, S. Diamond, N.S. Berke. *Steel Corrosion in Concrete: Fundamentals and Civil Engineering Practice*, first ed., Taylor & Francis, London, UK, 1997.
- [5] M.G. Alexander, H. Beushausen, Durability, service life prediction, and modelling for reinforced concrete structures – review and critique, *Cem. Concr. Res.* 122 (2019) 17–29, <https://doi.org/10.1016/j.cemconres.2019.04.018>.
- [6] E. Possan, W.A. Thomaz, G.A. Aleandri, E.F. Felix, A.C.P. dos Santos, CO₂ uptake potential due to concrete carbonation: a case study, *Case Stud. Constr. Mater.* 6 (2017) 147–161, <https://doi.org/10.1016/j.cscm.2017.01.007>.
- [7] M. Cyr, Influence of supplementary cementitious materials (SCMs) on concrete durability, in: *Eco-Efficient Concr*, Elsevier, 2013, pp. 153–197.
- [8] S. von Greve-Dierfeld, B. Lothenbach, A. Vollpracht, B. Wu, B. Huet, C. Andrade, C. Medina, C. Thiel, E. Gruyaert, H. Vanoutrive, I.F. Saéz del Bosque, I. Ignjatovic, J. Elsen, J.L. Provis, K.L. Scrivener, K.-C. Thienel, K. Sideris, M. Zajac, N.M. Alderete, Ö. Cizer, P. Van den Heede, R.D. Hooton, S. Kamali-Bernard, S.A. Bernal, Z. Zhao, Z. Shi, N. De Belie, Understanding the carbonation of concrete with supplementary cementitious materials: a critical review by RILEM TC 281-CCC, *Mater. Struct.* 53 (2020) 136, <https://doi.org/10.1617/s11527-020-01558-w>.
- [9] R. Loser, B. Lothenbach, A. Leemann, M. Tuchschnid, Chloride resistance of concrete and its binding capacity - comparison between experimental results and thermodynamic modeling, *Cem. Concr. Compos.* 32 (2010) 34–42, <https://doi.org/10.1016/j.cemconcomp.2009.08.001>.
- [10] L. Tang, L.-O. Nilsson, Chloride binding capacity and binding isotherms of OPC pastes and mortars, *Cem. Concr. Res.* 23 (1993) 247–253, [https://doi.org/10.1016/0008-8846\(93\)90089-R](https://doi.org/10.1016/0008-8846(93)90089-R).
- [11] Z. Shi, M.R. Geiker, K. De Weerd, B. Lothenbach, J. Kaufmann, W. Kunther, S. Ferreira, D. Herfort, J. Skibsted, Durability of portland cement blends including calcined clay and limestone: Interactions with sulfate, chloride and carbonate ions, *RILEM Book. 10* (2015) 133–141, https://doi.org/10.1007/978-94-017-9939-3_17.
- [12] P.-C. Aïtcin, S. Mindess, *Sustainability of Concrete*, CRC Press, 2011, <https://doi.org/10.1201/9781482266696>.
- [13] M.R.C. da Silva, C.S. Malacarne, M.A. Longhi, A.P. Kirchheim, Valorization of kaolin mining waste from the Amazon region (Brazil) for the low-carbon cement production, *Case Stud. Constr. Mater.* 15 (2021), <https://doi.org/10.1016/j.cscm.2021.e00756>.
- [14] K.L. Scrivener, Options for the future of cement, *Indian Concr. J.* 88 (2014) 11–21.
- [15] E.F. Irassar, A. Tironi, V.L. Bonavetti, M.A. Trezza, C.C. Castellano, V.F. Rahhal, H.A. Donza, A.N. Scian, Thermal treatment and pozzolanic activity of calcined clay and shale, *ACI Materials J.* 116 (2019) 133–143, <https://doi.org/10.14359/51716717>.
- [16] A. Trümer, H.M. Ludwig, M. Schellhorn, R. Diedel, Effect of a calcined Westerwald bentonite as supplementary cementitious material on the long-term performance of concrete, *Appl. Clay Sci.* 168 (2019) 36–42, <https://doi.org/10.1016/j.clay.2018.10.015>.
- [17] J. Skibsted, R. Snellings, Reactivity of supplementary cementitious materials (SCMs) in cement blends, *Cem. Concr. Res.* 124 (2019), 105799, <https://doi.org/10.1016/J.CEMCONRES.2019.105799>.
- [18] R.S. Almenares, L.M. Vizcaíno, S. Damas, A. Mathieu, A. Alujas, F. Martirena, Industrial calcination of kaolinic clays to make reactive pozzolans, *Case Stud. Constr. Mater.* 6 (2017) 225–232, <https://doi.org/10.1016/j.cscm.2017.03.005>.
- [19] A. Ito, R. Wagai, Global distribution of clay-size minerals on land surface for biogeochemical and climatological studies, *Sci. Data* 4 (2017), 170103, <https://doi.org/10.1038/sdata.2017.1031>.
- [20] P.E. Zalba, M.E. Morosi, M.S. Conconi, Gondwana industrial clays: Tandilia System, Argentina-geology and applications. First Edit, Springer, 2016, <https://doi.org/10.1007/978-3-319-39457-2>.
- [21] V.L. Bonavetti, H.A. Donza, M. Pappalardi, C. Milanese, D. Violini, E.F. Irassar, Performance de un nuevo cemento compuesto elaborado con puzolanas obtenidas por medio de arcilla calcinada y filler, in: V.L. Bonavetti (Ed.), VIII Congr. Int. - 22^a Reun. Técnica La Asoc. Argentina Tecnol. Del Hormigón, Asociación Argentina de Tecnología del Hormigón (AATH), Olavarría, Argentina, 2018, pp. 147–154.
- [22] N. Beuntner, Zur Eignung und Wirkungsweise calcinierter Tone als reaktive Bindemittelkomponente im Zement (On the suitability and effectiveness of calcined clays as reactive binder components in cement), Beuth Verlag GmbH, 2017.
- [23] M. Frías, J. Cabrera, Pore size distribution and degree of hydration of metakaolin-cement pastes, *Cem. Concr. Res.* 30 (2000) 561–569, [https://doi.org/10.1016/S0008-8846\(00\)00203-9](https://doi.org/10.1016/S0008-8846(00)00203-9).
- [24] A. Tironi, C. Castellano, V.L. Bonavetti, M.A. Trezza, A.N. Scian, E.F. Irassar, Kaolinic calcined clays - Portland cement system: hydration and properties, *Constr. Build. Mater.* 64 (2014) 215–221, <https://doi.org/10.1016/j.conbuildmat.2014.04.065>.
- [25] G. Marchetti, V.F. Rahhal, Z. Pavlík, M. Pavlíková, E.F. Irassar, Assessment of packing, flowability, hydration kinetics, and strength of blended cements with illitic calcined shale, *Constr. Build. Mater.* 254 (2020), 119042, <https://doi.org/10.1016/j.conbuildmat.2020.119042>.

- [26] N.S. Msinjili, N. Vogler, P. Sturm, M. Neubert, H.J. Schröder, H.C. Kühne, K.J. Hünger, G.J.G. Gluth, Calcined brick clays and mixed clays as supplementary cementitious materials: Effects on the performance of blended cement mortars, *Constr. Build. Mater.* 266 (2021), 120990, <https://doi.org/10.1016/j.conbuildmat.2020.120990>.
- [27] A. Alujas, R. Fernandez, R. Quintana, K.L. Scrivener, F. Martirena, Pozzolanic reactivity of low grade kaolinitic clays: influence of calcination temperature and impact of calcination products on OPC hydration, *Appl. Clay Sci.* 108 (2015) 94–101, <https://doi.org/10.1016/j.clay.2015.01.028>.
- [28] A. Tironi, M.A. Trezza, A.N. Scian, E.F. Irassar, Incorporation of calcined clays in mortars: porous structure and compressive strength, *Procedia, Mater. Sci.* 1 (2012) 366–373, <https://doi.org/10.1016/J.MSPRO.2012.06.049>.
- [29] N.S. Msinjili, G.J.G. Gluth, P. Sturm, N. Vogler, H.C. Kühne, Comparison of calcined illitic clays (brick clays) and low-grade kaolinitic clays as supplementary cementitious materials, *Mater. Struct. Constr.* 52 (2019), <https://doi.org/10.1617/s11527-019-1393-2>.
- [30] N. Beuntner, R. Sposito, K.-C. Thienel, Potential of calcined mixed-layer clays as pozzolans in concrete, *ACI Materials J.* 116 (2019) 19–29, <https://doi.org/10.14359/51716677>.
- [31] S. Scherb, N. Beuntner, M. Köberl, K.-C. Thienel, The early hydration of cement with the addition of calcined clay—From single phyllosilicate to clay mixture, in: H.-B. Fischer, A. Volke (Eds.), 20th Int. Build. Mater. Conf, F.A. Finger Institute for Building Materials Science, Weimar, 2018, pp. 658–666.
- [32] A. Tironi, M.A. Trezza, A.N. Scian, E.F. Irassar, Kaolinitic calcined clays: factors affecting its performance as pozzolans, *Constr. Build. Mater.* 28 (2012) 276–281, <https://doi.org/10.1016/j.conbuildmat.2011.08.064>.
- [33] G. Cordoba, S.V. Zito, R. Sposito, V.F. Rahhal, A. Tironi, K.-C. Thienel, E.F. Irassar, Concretes with calcined clay and calcined shale: workability, mechanical, and transport properties, *J. Mater. Civ. Eng.* 32 (2020), 4020224, [https://doi.org/10.1061/\(ASCE\)MT.1943-5533.0003296](https://doi.org/10.1061/(ASCE)MT.1943-5533.0003296).
- [34] K.L. Scrivener, R. Snellings, B. Lothenbach, A Practical Guide To Microstructural Analysis of Cementitious Materials, Taylor & Francis Group, 2018, <https://doi.org/10.1201/b19074>.
- [35] S. Mindess, J.F. Young, D. Darwin, *Concrete, second ed.*, Prentice Hall, 2003.
- [36] L. Basheer, J. Kropp, D.J. Cleland, Assessment of the durability of concrete from its permeation properties: a review, *Constr. Build. Mater.* 15 (2001) 93–103, [https://doi.org/10.1016/S0950-0618\(00\)00058-1](https://doi.org/10.1016/S0950-0618(00)00058-1).
- [37] M. Cyr, P. Lawrence, E. Ringot, Efficiency of mineral admixtures in mortars: quantification of the physical and chemical effects of fine admixtures in relation with compressive strength, *Cem. Concr. Res.* 36 (2006) 264–277, <https://doi.org/10.1016/j.cemconres.2005.07.001>.
- [38] J.M. Khatib, S. Wild, Pore size distribution of metakaolin paste, *Cem. Concr. Res.* 26 (1996) 1545–1553, [https://doi.org/10.1016/0008-8846\(96\)00147-0](https://doi.org/10.1016/0008-8846(96)00147-0).
- [39] A. Tironi, R. Sposito, G. Cordoba, S.V. Zito, V.F. Rahhal, K.-C. Thienel, E.F. Irassar, Influence of different calcined clays to the water transport performance of concretes, *Mag. Concr. Res.* (2021), <https://doi.org/10.1680/jmacr.21.00031>.
- [40] V.L. Bonavetti, Cementos con filler calcáreo - Mecanismo de interacción y su influencia sobre las propiedades resistentes, *Univ. Nac. Del. Cent. De. la Prov. De. Buenos Aires* (1998).
- [41] A. Lozano-Lunar, P.R. da Silva, J. de Brito, J.I. Álvarez, J.M. Fernández, J.R. Jiménez, Performance and durability properties of self-compacting mortars with electric arc furnace dust as filler, *J. Clean. Prod.* 219 (2019) 818–832, <https://doi.org/10.1016/j.jclepro.2019.02.145>.
- [42] N.M. Alderete, Y.A. Villagrán Zaccardi, D. Snoeck, B. Van Belleghem, P. Van den Heede, K. Van Tittelboom, N. De Belie, Capillary imbibition in mortars with natural pozzolan, limestone powder and slag evaluated through neutron radiography, electrical conductivity, and gravimetric analysis, *Cem. Concr. Res.* 118 (2019) 57–68, <https://doi.org/10.1016/j.cemconres.2019.02.011>.
- [43] I. De la Varga, J. Castro, D.P. Bentz, F. Zunino, J. Weiss, Evaluating the hydration of high volume fly ash mixtures using chemically inert fillers, *Constr. Build. Mater.* 161 (2018) 221–228, <https://doi.org/10.1016/j.conbuildmat.2017.11.132>.
- [44] A. Noushini, A. Castel, J. Aldred, A. Rawal, Chloride diffusion resistance and chloride binding capacity of fly ash-based geopolymer concrete, *Cem. Concr. Compos.* 105 (2020), 103290, <https://doi.org/10.1016/j.cemconcomp.2019.04.006>.
- [45] M. Sharma, S. Bishnoi, F. Martirena, K. Scrivener, Limestone calcined clay cement and concrete: a state-of-the-art review, *Cem. Concr. Res.* 149 (2021), 106564, <https://doi.org/10.1016/j.cemconres.2021.106564>.
- [46] Y. Dhandapani, M. Santhanam, Investigation on the microstructure-related characteristics to elucidate performance of composite cement with limestone-calcined clay combination, *Cem. Concr. Res.* 129 (2020), 105959, <https://doi.org/10.1016/j.cemconres.2019.105959>.
- [47] B. Johannesson, Transport and sorption phenomena in concrete and other porous media, *Lund. Univ.* (2000).
- [48] B.B. Sabir, S. Wild, J. Bai, Metakaolin and calcined clays as pozzolans for concrete: a review, *Cem. Concr. Compos.* 23 (2001) 441–454, [https://doi.org/10.1016/S0958-9465\(00\)00092-5](https://doi.org/10.1016/S0958-9465(00)00092-5).
- [49] D.V. Ribeiro, S.A. Pinto, N.S. Amorim Júnior, J.S. Andrade Neto, I.H.L. Santos, S.L. Marques, M.J.S. França, Effects of binders characteristics and concrete dosing parameters on the chloride diffusion coefficient, *Cem. Concr. Compos.* 122 (2021), <https://doi.org/10.1016/j.cemconcomp.2021.104114>.
- [50] L. Tang, L.-O. Nilsson, P.A.M. Basheer, Resistance of Concrete to Chloride Ingress: Testing and modelling, Taylor & Francis, Boca Raton, 2011.
- [51] B. Mobasher, M. Shekarchi, A. Bonakdar, M. Bakhshi, A. Mirdamadi, Transport properties in metakaolin blended concrete, *Constr. Build. Mater.* 24 (2010) 2217–2223, <https://doi.org/10.1016/j.conbuildmat.2010.04.035>.
- [52] J. Seo, S. Kim, S. Park, S.J. Bae, H.K. Lee, Microstructural evolution and carbonation behavior of lime-slag binary binders, *Cem. Concr. Compos.* 119 (2021), 104000, <https://doi.org/10.1016/j.cemconcomp.2021.104000>.
- [53] P.H.R. Borges, J.O. Costa, N.B. Milestone, C.J. Lynsdale, R.E. Streatfield, Carbonation of CH and C-S-H in composite cement pastes containing high amounts of BFS, *Cem. Concr. Res.* 40 (2010) 284–292, <https://doi.org/10.1016/j.cemconres.2009.10.020>.
- [54] C. Andrade, R. Buják, Effects of some mineral additions to Portland cement on reinforcement corrosion, *Cem. Concr. Res.* 53 (2013) 59–67, <https://doi.org/10.1016/j.cemconres.2013.06.004>.
- [55] M. Hren, V. Bokan Bosiljkov, A. Legat, Effects of blended cements and carbonation on chloride-induced corrosion propagation, *Cem. Concr. Res.* 145 (2021), 106458, <https://doi.org/10.1016/j.cemconres.2021.106458>.
- [56] Q. Shen, G. Pan, B. Bao, Influence of CSH carbonation on the porosity of cement paste, *Mag. Concr. Res.* 68 (2016) 504–514, <https://doi.org/10.1680/jmacr.15.00286>.
- [57] A. Trümer, H.M. Ludwig, Assessment of calcined clays according to the main criterions of concrete durability, in: RILEM Bookseries, Springer, Netherlands, 2018, pp. 475–481, https://doi.org/10.1007/978-94-024-1207-9_76.
- [58] B. Johannesson, P. Utgenannt, Microstructural changes caused by carbonation of cement mortar, *Cem. Concr. Res.* 31 (2001) 925–931, [https://doi.org/10.1016/S0008-8846\(01\)00498-7](https://doi.org/10.1016/S0008-8846(01)00498-7).
- [59] G.K. Glass, N.R. Buenfeld, The presentation of the chloride threshold level for corrosion of steel in concrete, *Corros. Sci.* 39 (1997) 1001–1013, [https://doi.org/10.1016/S0010-938X\(97\)00009-7](https://doi.org/10.1016/S0010-938X(97)00009-7).